Comparison of Lithium Granule Induced ELM triggering threshold levels for EAST and DIII-D

R. Lunsford[1], Z. Sun[2], A. Bortolon1, J. S. Hu[2], R. Maingi[1], D. K. Mansfield[1], A. Nagy[1]
and the EAST and DIII-D Teams

[1]Princeton Plasma Physics Laboratory, Princeton, N. J. 08543, USA
[2]Institue of Plasma Physics, Chinese Academy of Sciences, Hefei, Anhui 230031, China

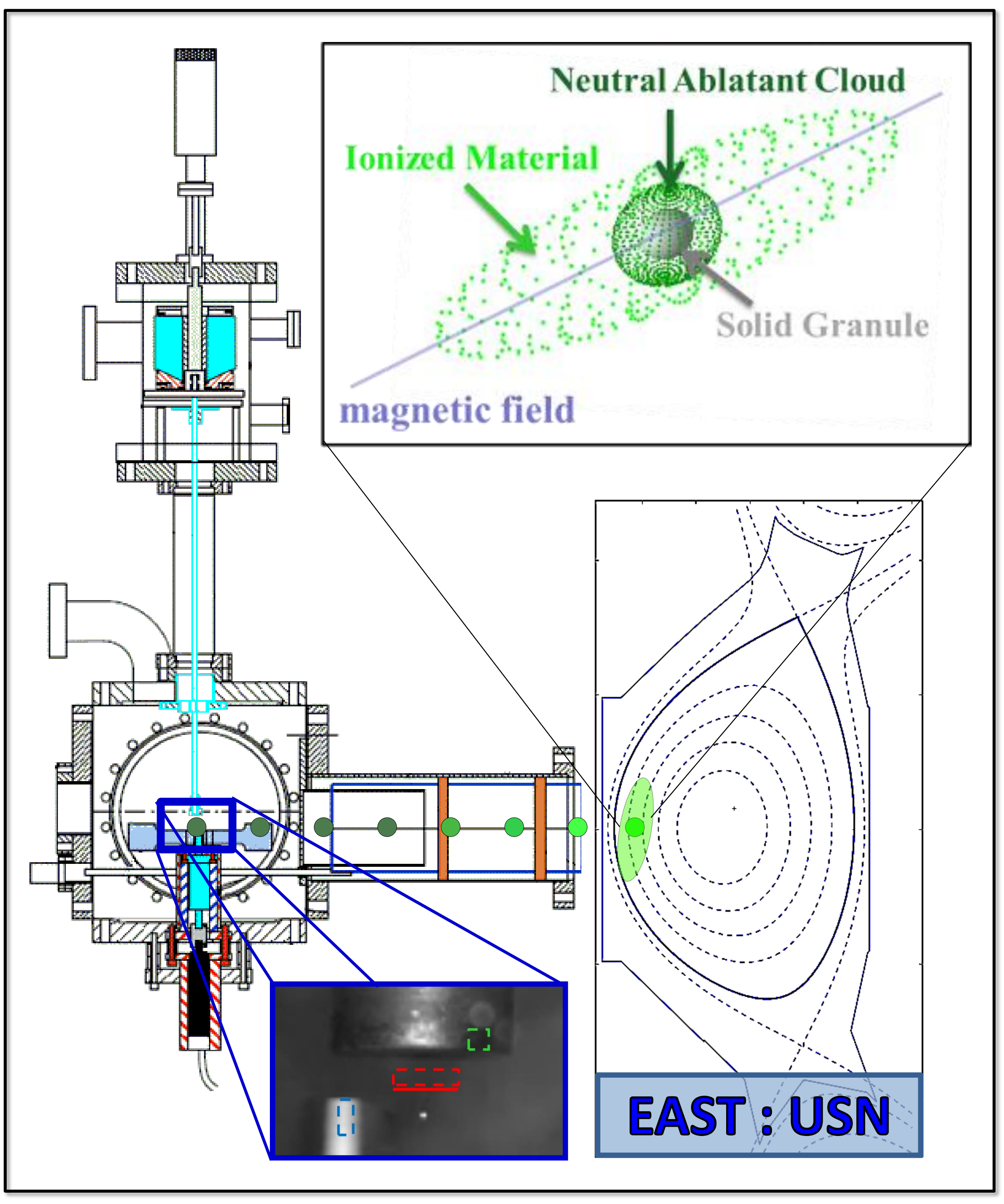

Overview

- ELM pacing is a baseline mitigation strategy for ITER
- To achieve pacing with granules there must be a high probability of triggering an ELM
- The injector horizontally drives impurity microgranules ranging in diameter from 200 – 1000 microns radially into the low field side of the discharge.
- Granule size selected between shots by selecting between reservoirs accessed by rotational feedthrough
- Granules are tracked through multiple cameras and other diagnostics to determine ELM triggering probability
- Future experiments will measure the ELM pacing factor achieved when the frequency is driven above its baseline level.

Pacing ELMs can reduce peak heat flux

- ELM intensity observed to be inversely proportional to ELM frequency

$$\Delta W_{ELM} \times f_{ELM} \sim const$$

- Rapid triggering of ELMs should lead to a reduction in the peak ELM intensity.
- Paced ELM heat fluxes reduced to a level more tractable to the plasma facing components.
- This effect has been seen in deuterium pellet pacing and with lithium granule pacing in DIII-D hybrid scenarios (shown at right)
- The heat flux reduction is less pronounced in similar experiments in JET-ILW, AUG, and DIII-D ITER baseline scenarios, necessitating further study.

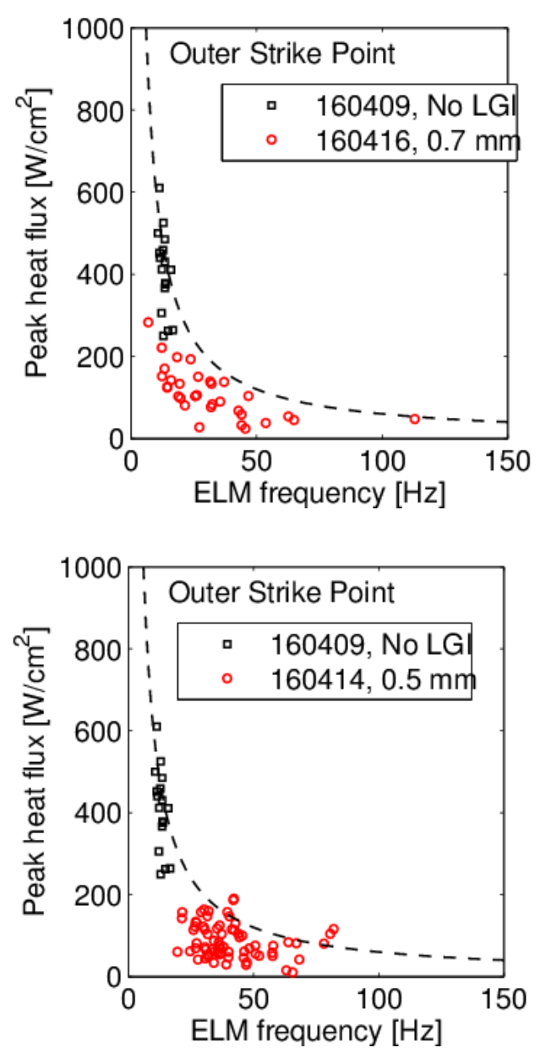

Neutral Gas Shielding Model of Granule Ablation

$$4\pi\, r_g{}^2\, q_s = G[\Delta H + T_C(1 + {}^5\!/_6\, M_C{}^2) + {}^3\!/_2\,(T_C - T_S)] + Q_{inv}$$

$$-\frac{dr_g}{dt} = \frac{\eta f_B f_L q_S}{n_0\left[\Delta H + T_S\left(\frac{5}{2} + \frac{5}{6} M_C{}^2\right)\right]}$$

Adapted from P. B. Parks et al. NF 34 (1994) &
G. Kocsis et al. PPCF 41 (1999)

r_g = Granule Radius
ΔH = Sublimation Energy (Li = 1.6 eV/atom)
T_C = Cloud Temperature ($T_C = 0.7T_S$)
T_S = Surface Temperature (T_S = 0.14 eV - Li Boil Point)
M_C = Cloud Mach Number (M_C = 1, sonic flow)

η = Cloud Shielding Parameter
f_B = Field directed heating anisotropy (~1/2)
f_L = Flux Screening Parameter (0.16 for H_2, 1 if no screening)
n_g = Granule Density

$$Q_{inv} = cm_p \frac{d}{dt}\, T_s$$

We assume that the surface temperature rapidly equilibrates so that this term can be neglected

Ablation Rate of the Injected Granule

$$G = \frac{4\pi r_g{}^2 q_s \eta f_B}{n_g}\left[\Delta H + \frac{10}{3} T_S\right]^{-1} \qquad q_s = \frac{1}{2}\, n_e T_e \left(\frac{8T_e}{\pi m_e}\right)^{1/2}$$

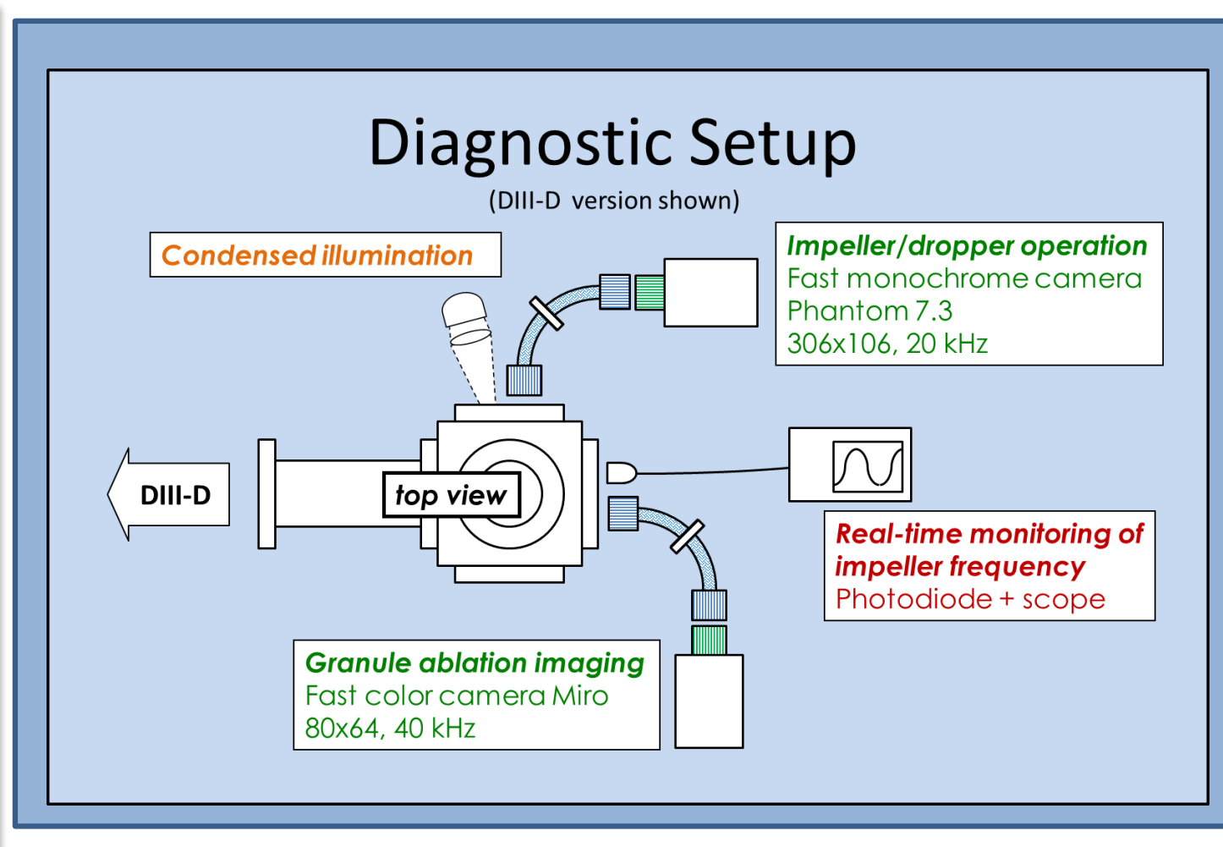
Diagnostic Setup
(DIII-D version shown)

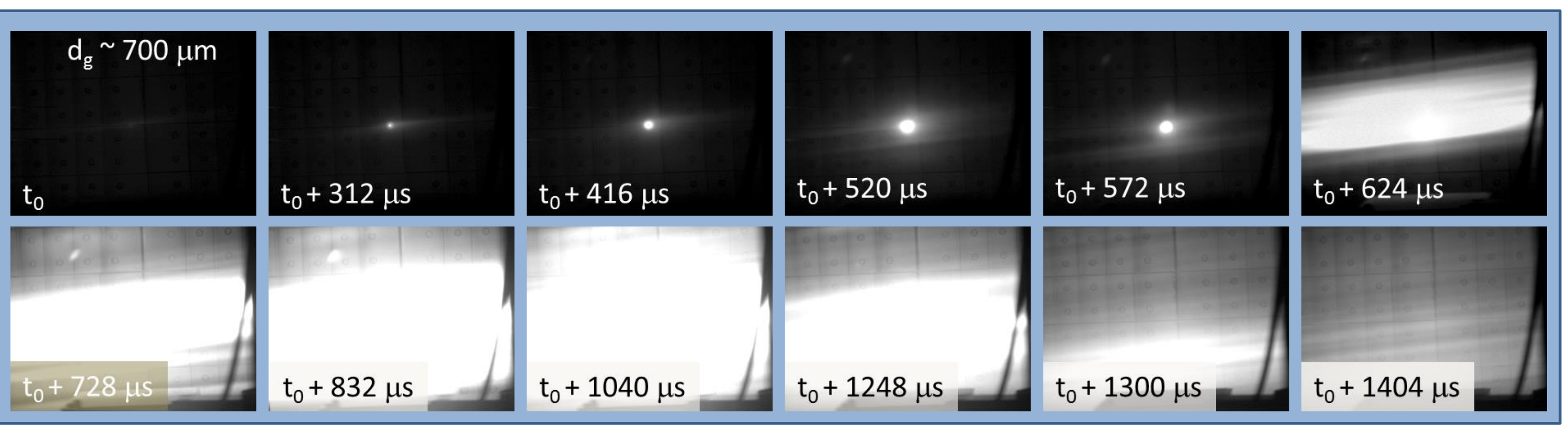

Camera images recorded radially inward along granule injection path

- High energy electron influx sublimates pellet surface generating a high density neutral cloud with a radius 2-4x the granule diameter
- Heat transfer ionizes the cloud which streams along field lines and the ablation rate of the shielded granule is controlled by the neutral cloud
- Granule ablation generates an overdense flux tube, if past a threshold, this additional pressure can drive an MHD ballooning-type instability, triggering an ELM.

DIII-D Triggering Efficiency

W_{MHD} = 600 kJ
I_P = 1.2 MA

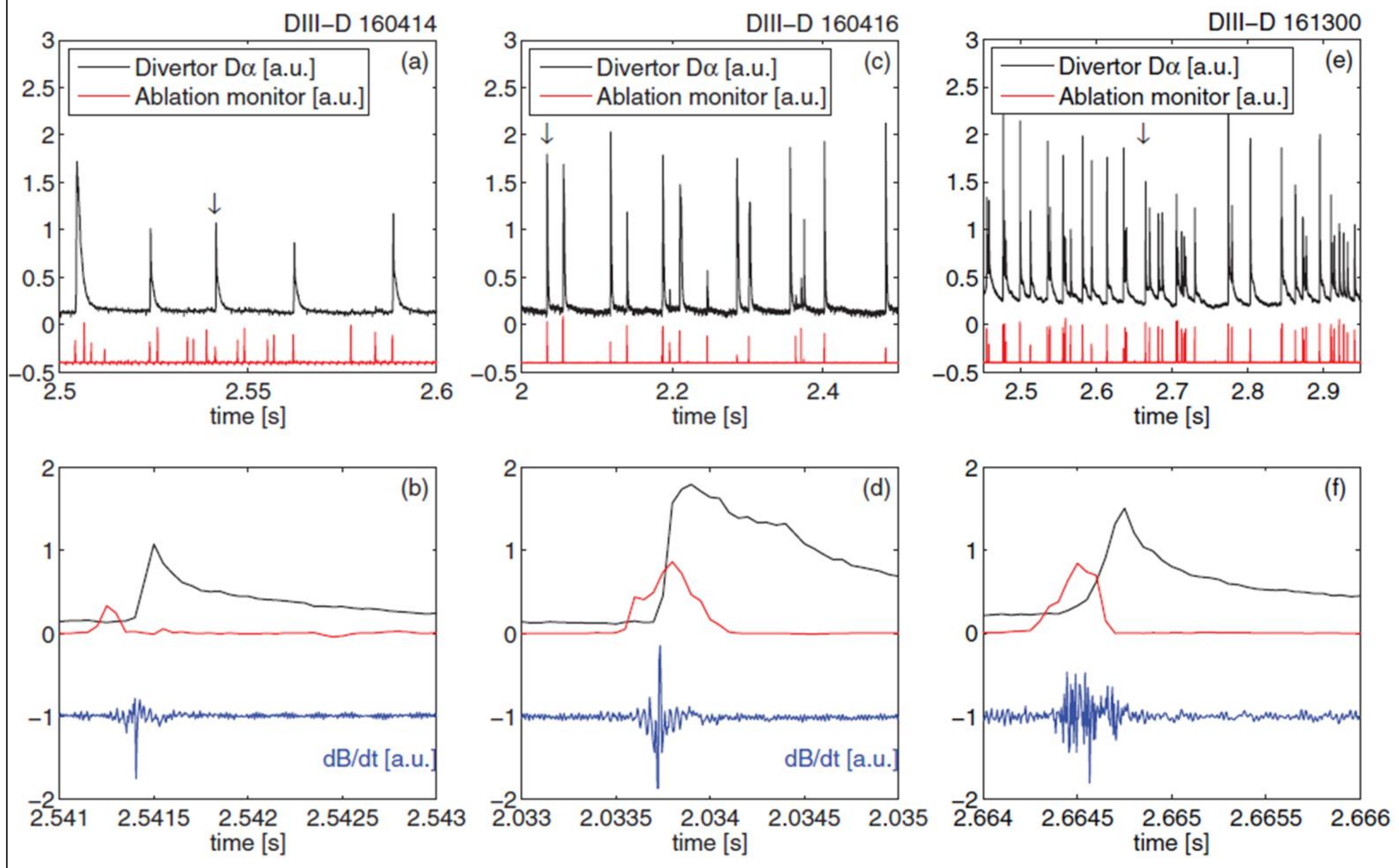

d_G ≈ 400 microns f_G ≈ 140 Hz T_G ~ 15 - 30%	d_G ≈ 700 microns f_G ≈ 60 Hz T_G ~ 70 - 90%	d_G ≈ 900 microns f_G ≈ 100 Hz T_G ~ 95%+

EAST Triggering Efficiency

W_{MHD} = 175 kJ
I_P = 400 kA

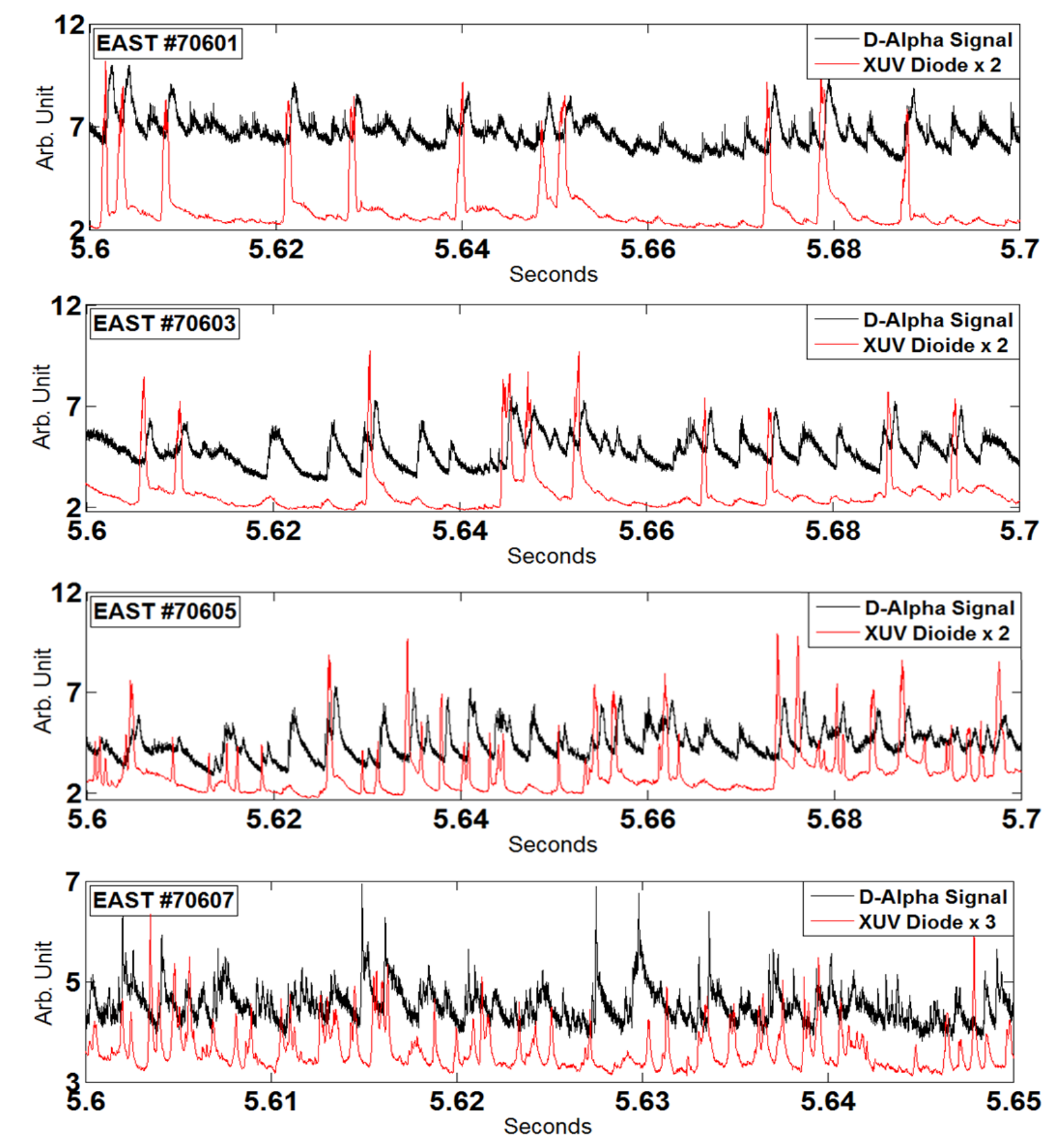

d_G ≈ 900 microns
f_G ≈ 110 Hz
T_G = 100%

d_G ≈ 700 microns
f_G ≈ 100 Hz
T_G ~ 95% +

d_G ≈ 500 microns
f_G ≈ 300 Hz
T_G ~ 50 - 90%

d_G ≈ 300 microns
f_G ≈ 500 Hz +
T_G ~ 10 - 30%

1. Granules are tracked from dropper tube exit, through impact with the impeller, into the discharge
2. Multiple velocity measurements confirm time of flight to match injection with ablation events
3. Signal from ablation camera compared to mainline diagnostics : XUV(EAST) and dB/dt (DIII-D)
4. If peak on diagnostic trace matches ELM peak on Dα trace, granule is assumed to have triggered the ELM
5. There is the possibility for natural ELMs to be concurrent with granule injection, so these values are an upper bound

NGS model used to determine DIII-D ablatant deposition

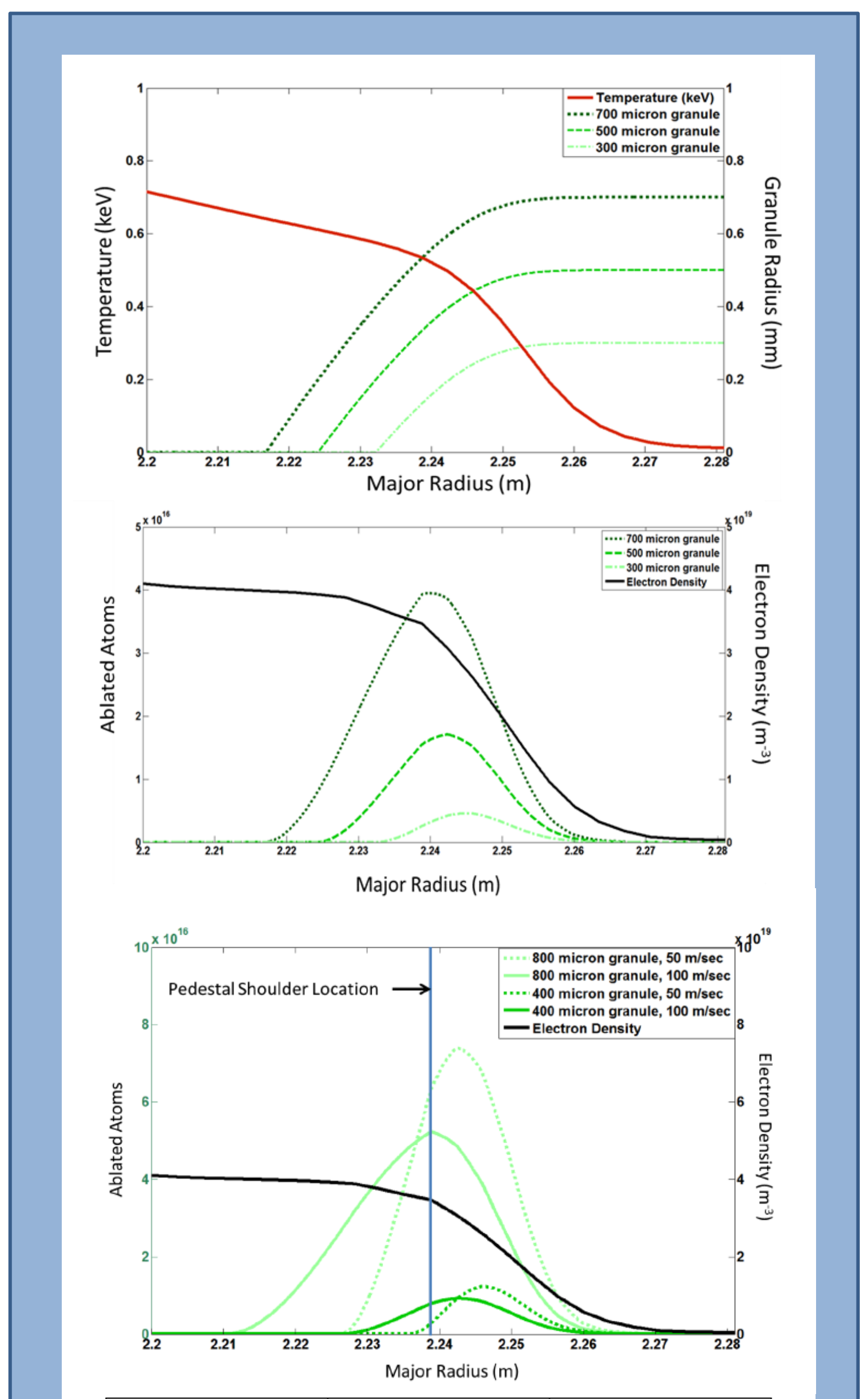

Granule Size	Granule Velocity	Atoms deposited atop the pedestal
400 microns	50 m/sec	3.68×10^{16}
400 microns	100 m/sec	4.11×10^{17}
600 microns	50 m/sec	7.54×10^{17}
600 microns	75 m/sec	1.66×10^{18}
600 microns	100 m/sec	2.31×10^{18}
600 microns	125 m/sec	2.77×10^{18}
800 microns	50 m/sec	3.29×10^{18}
800 microns	100 m/sec	6.85×10^{18}

Table 1 : Mass deposition located past the pedestal shoulder for a range of injection sizes and velocities

ELM triggering correlates to atoms deposited at the top of the pedestal

Triggering > 80% occurs above ~2 x 10^{18}

ELM Triggering vs Granule Size

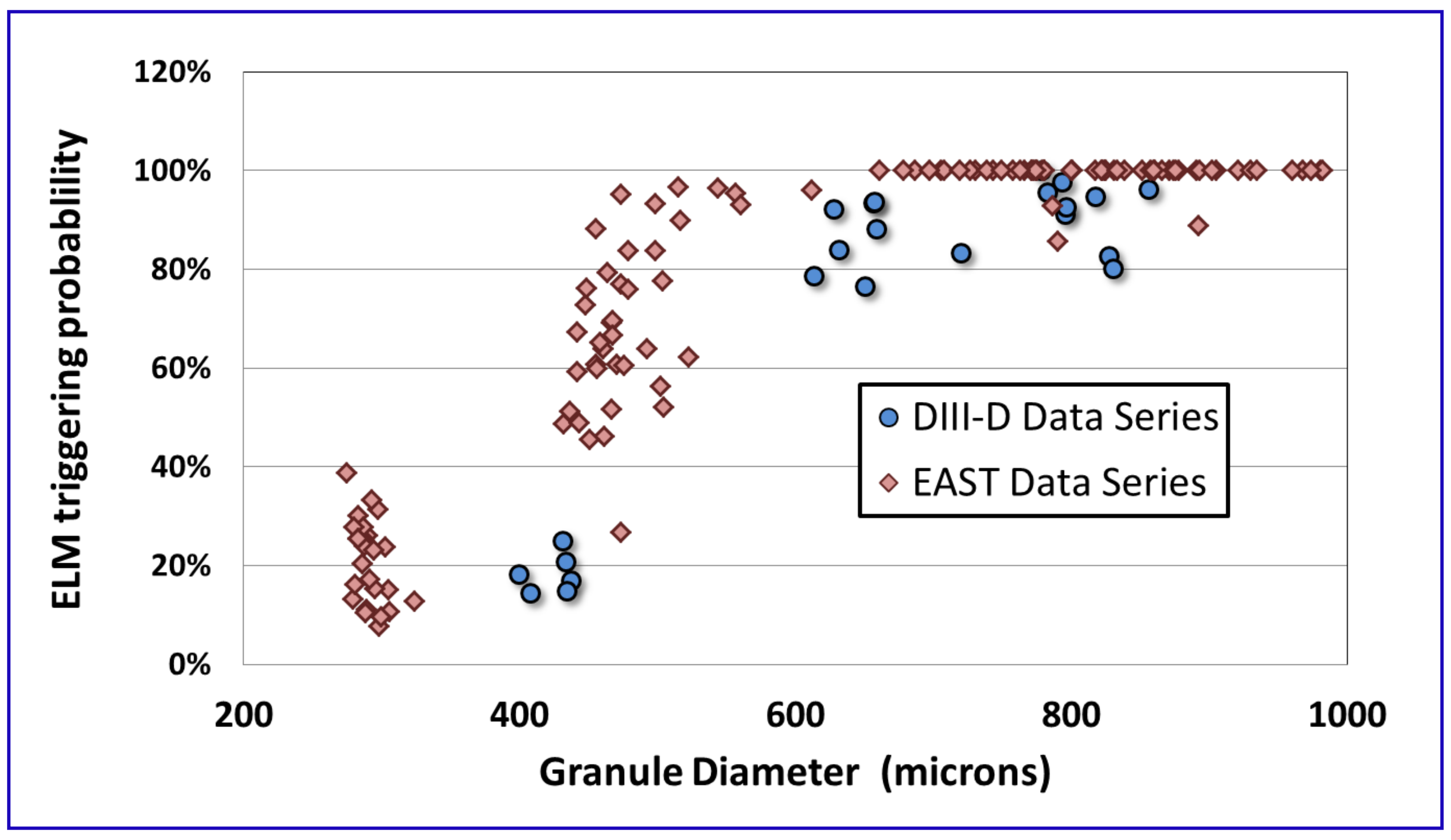

1. Each data point represents an aggregate size and triggering efficiency for a small time window
2. Both machines show similar if distinct trends with DIII-D triggering efficiencies lower than equivalent EAST granule injections
3. Variations in triggering efficiency for EAST ~500 micron granules are the result of coupling the granule injection into the nominal ELM cycle of the discharge

Conclusions

1. Distinct granule size threshold has been observed on both DIII-D and EAST with similar characteristic behavior
2. Triggering threshold on EAST slightly lower than on DIII-D, most likely due to lower edge temperatures and densities allowing greater granule penetration
3. Dual-machine comparison begins to suggest scaling laws for solid granule triggering threshold, applicable to next step devices

Further Research

1. Simulation of granule injection into EAST discharges to determine ablatant deposition and pedestal penetration
2. Analysis of alternate injection materials (B, BN, B_4C, C) to determine species specific triggering efficiencies
3. Injection experiments with EAST full W divertors to assess PMI triggering effect
4. Characterization of near simultaneous injection of 300 micron granules to determine edge conditioning effects
5. Examination of multi-species impurity transport effects using both powder dropper and granule injector